Available online at www.sciencedirect.com
ScienceDirect
Ceramics International 36 (2010) 451–457
CERAMICS INTERNATIONAL
www.elsevier.com/locate/ceramint

Microstructural characterization of spark plasma sintered boron carbide ceramics

S. Hayun, S. Kalabukhov, V. Ezersky, M.P. Dariel, N. Frage *

Department of Materials Engineering, Ben-Gurion University of the Negev, P.O. Box 653, Beer-Sheva 84105, Israel

Received 16 May 2009; received in revised form 9 July 2009; accepted 20 August 2009
Available online 22 September 2009

Abstract

Fully dense boron carbide specimens were fabricated by the spark plasma sintering (SPS) technology in the absence of any sintering additives. Densification starts at 1500 °C and the highest densification rate is reached at about 1900 °C. The microstructure of the ceramic sintered at 2200 °C, with heating rates in the 50–400 °C/min range, displays abnormal grain growth, while for a 600 °C/min heating rate a homogeneous distribution of finely equiaxed grains with 4.05 ± 1.62 μm average size was obtained. TEM analysis revealed the presence of W-based amorphous and of crystalline boron-rich $B_{50}N_2$ secondary phases at triple-junctions. No grain-boundary films were detected by HRTEM. The formation of a transient liquid alumino-silicate phase stands apparently behind the early stage of densification.

Keywords: Boron carbide; Spark plasma sintering (SPS); Sintering behaviour; Microstructure; TEM; HRTEM

1. Introduction

Boron carbide (B_4C) is a promising material for a variety of applications that require elevated mechanical properties [1–10]. The realization of this potential is hindered by the very high temperature required for sintering, on account of the covalent bonding that prevails in boron carbide [11]. A sintering schedule at that elevated temperatures leads to rapid grain coarsening [12,13] and is an expensive processing approach. In order to alleviate this problem, the sintering of boron carbide is commonly performed with free carbon as a sintering additive. Schwetz and Grellner [14] have shown that adding 1–3 wt% of excess free carbon to the boron carbide powder with a specific surface area higher than 15 m^2/g, allows fabricating sintered bodies with a relative density above 95% and with a finely grained microstructure. The sintering additives, however, which usually appear as secondary phases, significantly affect the mechanical properties of the sintered ceramic. Recently, attempts were made to apply the relatively novel spark plasma sintering technique for fabricating fully dense B_4C specimens [15–18]. A maximal relative density of about 99.2% was attained by Dipankar et al. [16] in specimens with an initial particle size of 800 nm. In the present study, we conducted a systematic investigation of the sintering behavior and the microstructural features of boron carbide, processed by the SPS approach and in the absence of any sintering additive.

2. Experimental procedure

2.1. Starting materials and experimental set-up

Boron carbide powder HS grade (see Table 1), supplied by H.C. Starck Company was inserted into a graphite die (inner diameter 20 mm, outer diameter 40 mm), which was covered with 20 mm thick graphite wool for thermal insulation (Fig. 1). The die was placed into a SPS apparatus (type HP D5/1, FCT System, Rauenstein, Germany) equipped with a 50 kN uniaxial press. The sintering procedure was conducted in the 1800–2200 °C temperature range in a vacuum of 10^{-2} torr and under 32–51 MPa pressure. The heating rate was varied in the 50–600 °C/min range and the holding time at the highest temperatures was 0–10 min. The cooling rate at the peak temperature 1000 °C was 100 °C/min. A typical temperature and pressure regime over the densification cycle is shown in Fig. 2.

* Corresponding author. Tel.: +972 8 6479441; fax: +972 8 6489441.
E-mail address: nfrage@bgu.ac.il (N. Frage).

0272-8842/$36.00
doi:10.1016/j.ceramint.2009.09.004

Table 1
Powder characteristics.

Specific surface area	15–20 m^2/g
Particle size	
≤3 mm	90%
≤0.8 mm	50%
≤0.2 mm	10%
Impurity levels	
N	0.7 wt%
O	1.7 wt%
Fe	0.05 wt%
Si	0.15 wt%
Al	0.05 wt%
Other (Ca, Cr, Mg, Mn, Ni, Ti, W)	0.5 wt%
Total boron	75.05 wt%
Total carbon	21.8 wt%
B:C ratio	3.7–3.8%

2.2. Density and microstructural characterization

The density of the sintered bodies was determined by the liquid displacement method in distilled water. The microstructure was studied using electron microscopy: scanning electron microscopy (SEM, JEOL-35) in conjunction with an energy-dispersive spectrometer (EDS). Transmission electron microscopy (TEM) characterization was carried out on Tecnai F20 G2 and on JEOL FasTEM 2010 microscopes equipped with the Noran energy-dispersive spectrometer (EDS) for microprobe elemental analysis. The samples for the SEM characterization were prepared using standard metallographic procedures that included a last stage of polishing with 1 μm diamond paste. Polished sections were electro-chemically etched with a solution of KOH. TEM and STEM samples were prepared as follows: 1 mm thick foils were cut using 0.4 mm diamond saw and ground down to 500 μm. Disks of 3 mm diameter were drilled with cooper drill pipe and 40 μm diamond paste, ground down to 70 μm thickness, glued to a Cu support and polished to 30 μm thickness. Final thinning to electron transparency was carried out with a Gatan™ model 691 precision ion polishing system until perforation.

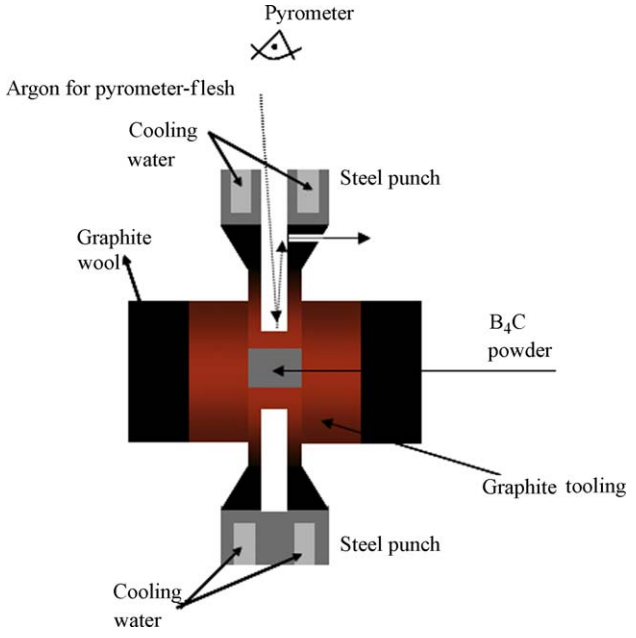

Fig. 1. Schematic set-up of SPS tools.

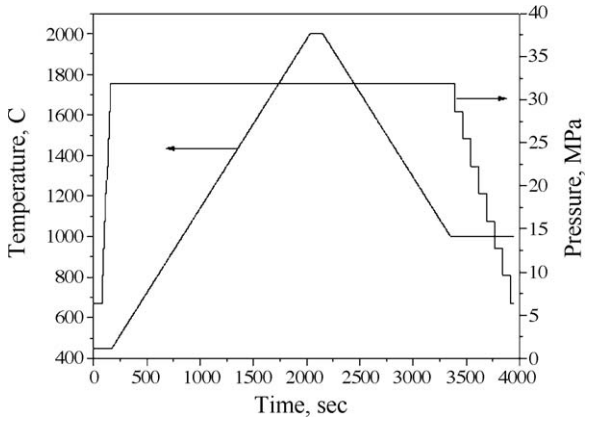

Fig. 2. A typical temperature and pressure program for SPS apparatus.

3. Results and discussion

3.1. The sintering behavior of boron carbide

The densification behavior of the boron carbide powder may be derived from the lower punch relative displacement curve (RPD). The RPD curve of the SPS process at a heating rate 50 °C/min is presented in Fig. 3a (line B) and corresponds to the superposition of displacements toward negative values, on account of the thermal expansion of the graphite tool and of the sample during heating, and toward the positive direction due to sample densification at elevated temperature and the thermal shrinkage during cooling. A calibration run using the same tool set-up with a fully dense sample was performed (line A, Fig. 3a), in order to separate the effect of the thermal expansion of the graphite parts and the densification of the B_4C powder (line C, Fig. 3a). A similar procedure was performed for a heating rate of 400 °C/min (Fig. 3b). According to these figures, in both cases the densification process starts at 1500 °C and the maximum densification rate is reached at about 1900 °C.

The effect of various parameters on the density of the sintered samples is shown in Fig. 4. As expected, with increasing the sintering temperature (Fig. 4a), holding time and applied pressure (data presented for sintered temperature 1900 °C) (Fig. 4b and c) the density of the SPS processed samples increases.

At the same time, a slight density decrease of the sample after heating up 2200 °C (without holding) was observed for a heating rate increase from 50 to 600 °C/min (Fig. 4d). This feature is attributed to the total time duration (9, 3.75 and 3.5 min for heating rates of 50, 400 and 600 °C/min, respectively) of the samples in the 1900–2200 °C temperature range during heating and cooling, the temperature interval in

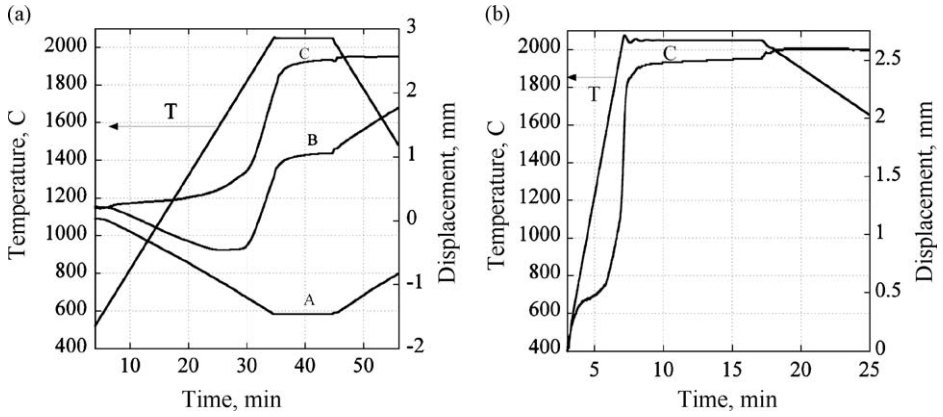

Fig. 3. RPD curves: (a) curve A corresponds to the run with fully dense sample, curve B corresponds to the run with B_4C powder and curve C represents the effect of densification. The presented data correspond to the heating rate of 50 °C/min and (b) RPD curve corresponds to the heating rates of 400 °C/min.

the course of which most of the densification process takes place.

According to the experimental results, a relative density of about 98% may be obtained by an SPS treatment at 2050 °C for 6 min with a heating rate of 50 °C/min under applied pressure of 32 MPa The fully dense specimens (density of 2.520 ± 0.012 g/cm^3) were fabricated under the same conditions with a holding time of 10 min. As shown below, the treatment at higher temperature leads to significant grain coarsening.

3.2. The microstructure of the sintered specimens

3.2.1. SEM characterization

The microstructure of fully dense boron carbide processed by SPS at 2050 °C/min for 10 min is shown in Fig. 5. The microstructure displays a homogeneous distribution of fine equiaxed grains with an average size of 4.05 ± 1.62 μm. The bright contrast of the grain boundaries (GB) is believed to be due to GB grooving caused by etching. The apparent porosity in

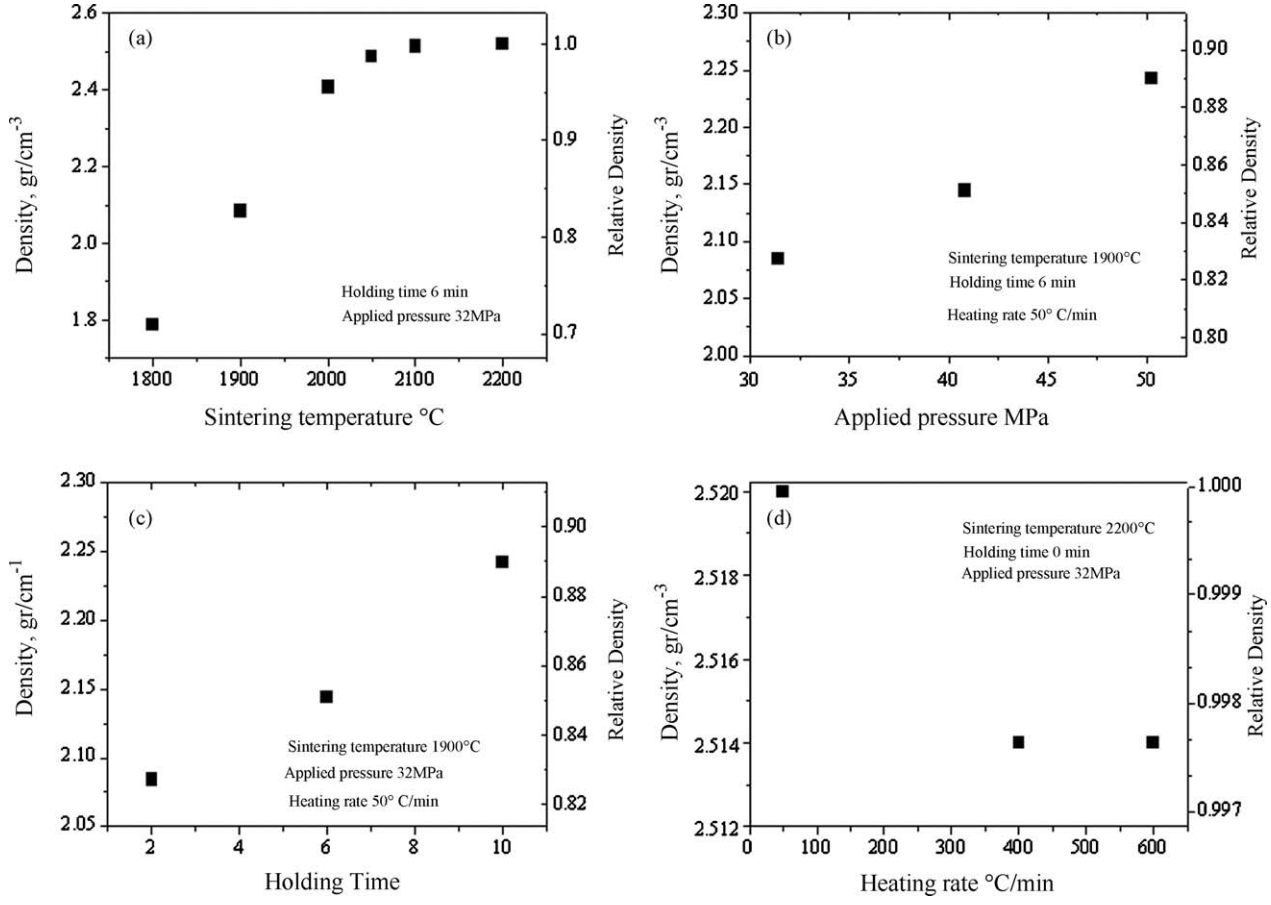

Fig. 4. The effect of various sintering parameters on the relative density of boron carbide specimens.

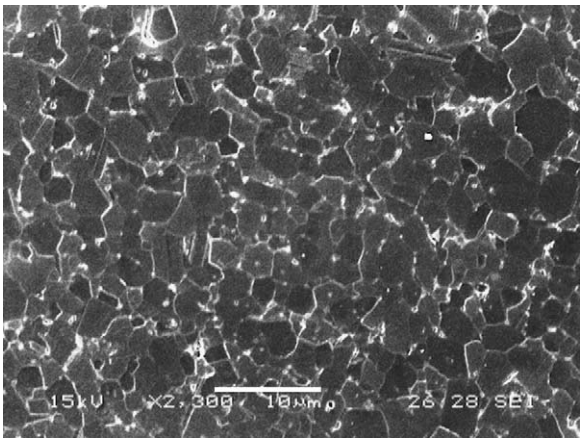

Fig. 5. The microstructure of the boron carbide processed by SPS at 2050 °C for 10 min.

the micrograph originates from the sample preparation procedure (polishing and etching) employed for metallographic characterization.

The effect of the heating rate on coarsening during treatments at 2200 °C and with no holding time is shown in Fig. 6. For the heating rates 50 and 400 °C/min, an abnormal grain growth was observed, while for the samples, which were heated at 600 °C/min, the microstructure was similar to that for samples hold at 2050 °C for 10 min. The experimental results related to the grain growth phenomenon as a function of heating rate are in good agreement with the results reported by Dole et al. [12] for hot-pressed boron carbide.

3.2.2. TEM characterization

TEM analysis was conducted in order to characterize the grain-boundary structure of the SPS processed boron carbide. The TEM image (Fig. 7) shows straight and sharp grain boundaries and confirms the results of the SEM investigation regarding the boron carbide grain size within the fully dense samples (Fig. 5). The presence of sub-micrometer particles at the grain boundaries and, in particular, at the triple-junctions, can be detected. EDS analysis of these particles at higher magnification and their electron diffraction images allow discerning the presence of two major particle types: (a) amorphous rectangular-shaped particles enriched with W, Fe, C and Ti and (b) plate-like shaped and crystalline particles. The latter are enriched with B and N and were attributed to the $B_{50}N_2$ phase [19] (Fig. 8). These particles originate from the impurities present in the boron carbide powder.

The presence of secondary phases at the GB of boron carbide processed by hot pressing, has been reported by Chen et al. [20]. The authors suggested that the presence of impurities or/and sintering aids contribute to the densification process by forming a secondary liquid phase in the course of the hot pressing process. In the SPS process, densification also starts at about 1500 °C (Fig. 3) and is also due to the formation of a secondary liquid phase. In order to verify the presence of the secondary phase, the grain-boundary structure was scrutinized closely. A bright field image of a high-angle grain-boundary is shown in Fig. 9. The selected area electron diffraction (SAED) that was taken from the grain-boundary shows the superposition of diffraction patterns of the boron carbide grains only and no evidence for the presence of any other phase.

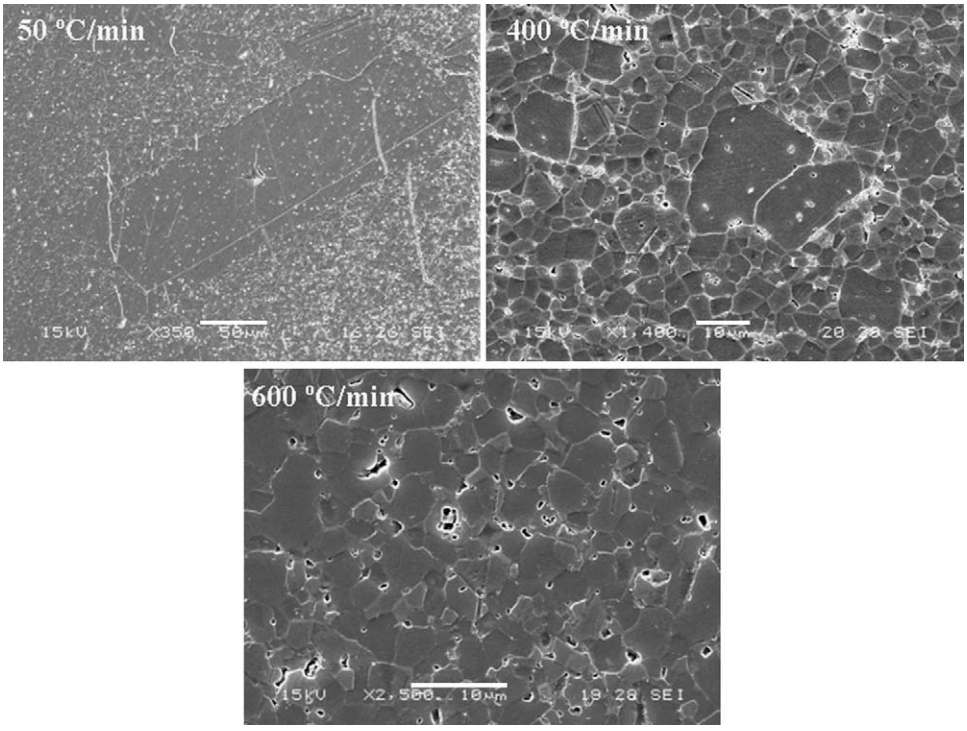

Fig. 6. SEM micrograph of boron carbide obtained at 2200 °C with heating rates of 50, 400 and 600 °C/min, with no holding time. Abnormal grain growth is observable in samples, which were fabricated at a heating rate of 50 and 400 °C/min.

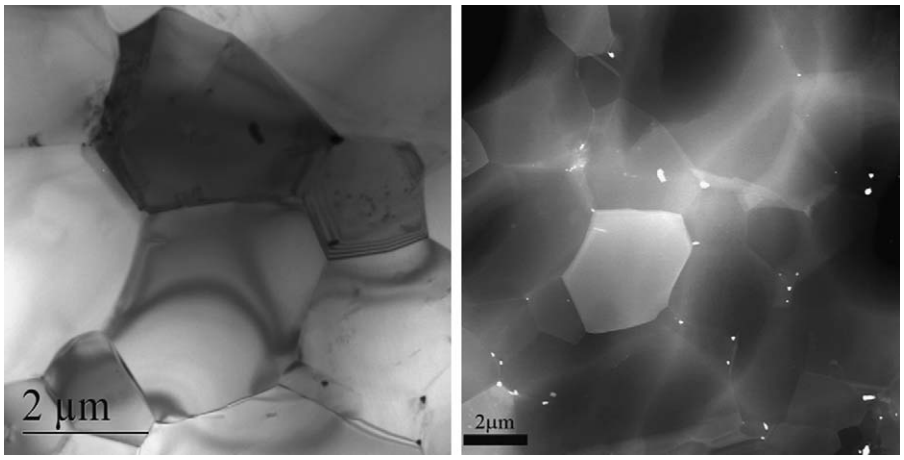

Fig. 7. TEM and STEM bright field image of a secondary phase at the triple-junction of the B_4C particles.

High resolution TEM images were obtained from the same area (Fig. 10). Both grains clearly display lattice fringes up to the boundary and with no evidence for any grain-boundary phase or amorphous film presence. The appearance of the relatively wide (2–3 nm) grain-boundary in Fig. 10b is due to the inclination of the boron carbide interface with respect to the observation zone axes. On the basis of the HRTEM observations and EDS analysis, we concluded that the grain boundaries in the SPS processed boron carbide are clean with no evidence for the presence of secondary phase films.

Covalent ceramic and boron carbide, in particular, are difficult to sinter to high relative density (>99%) without using at least a small amount of sintering additives [1,20,21]. In hot-pressed ceramics such as SiC [22,23], the presence of amorphous grain-boundary films with a thickness of about several atomic layers was observed. In HP boron carbide, however, no grain-boundary films were observed [20]. Nevertheless, the presence of impurities in particular Si and Al, evidently, affects the sintering behavior and induces the start of the densification process at 1500 °C (Fig. 3). This stage of the densification may be attributed to the formation of a transient alumino-silicate liquid phase that allows some particle rearrangement. At higher temperature, this liquid phase reacts with carbon that originated from the boron carbide, partial reduction of the oxides takes place and volatile sub-oxides SiO and Al_2O escape from the partially sintered samples. As a result of the reduction processes, free boron is released and forms the stable high temperature boron-rich phase, detected by TEM.

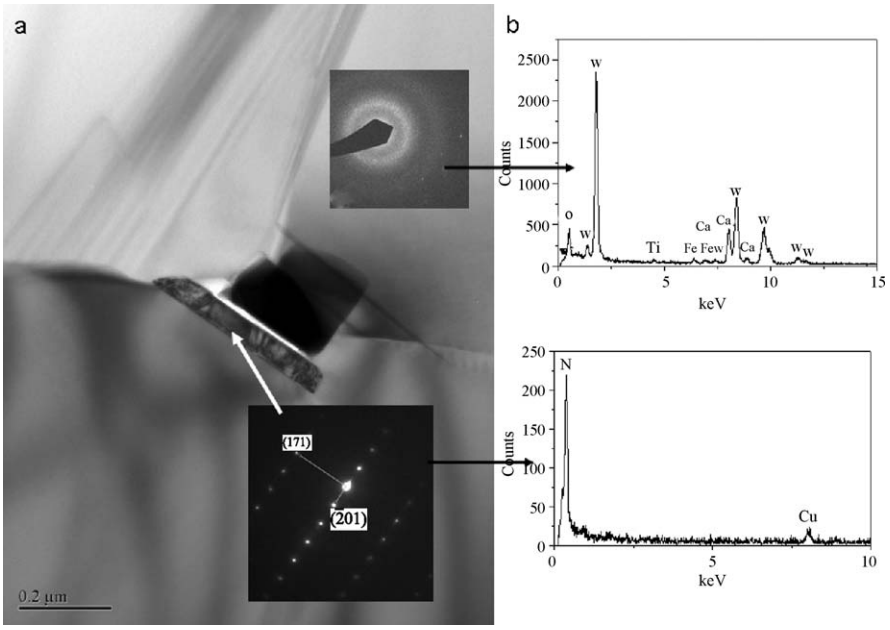

Fig. 8. Typical shapes of the secondary phases at the GB and triple-junctions (a) and their compositions; (b) the presence of Cu in the EDS analysis is attributed to the Cu grid that supports the boron carbide sample.

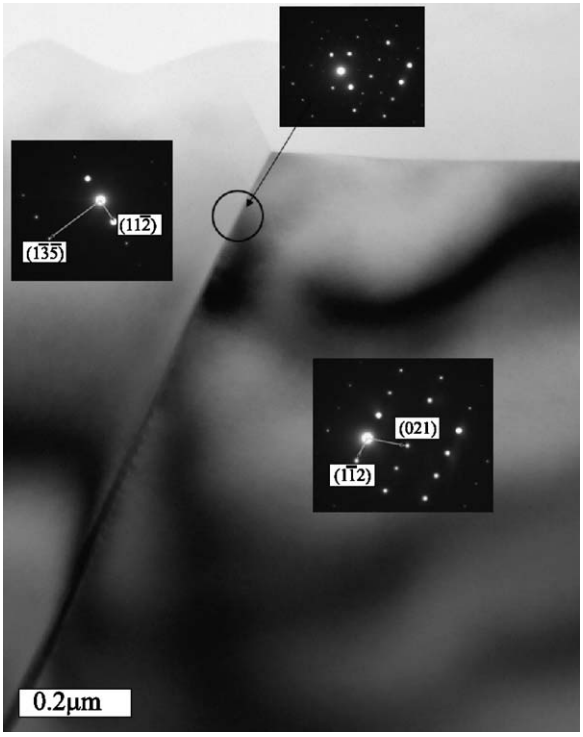

Fig. 9. Bright field TEM image of a high-angle grain-boundary in SPS processed boron carbide.

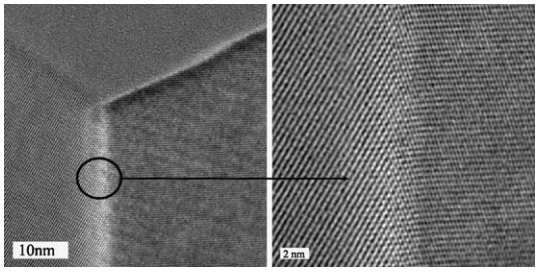

Fig. 10. Typical HRTEM images from the grain-boundary presented in Fig. 9.

4. Summary

Fully dense boron carbide specimens were fabricated by spark plasma sintering technology in the absence of any sintering additives. The densification behavior of the boron carbide powder was derived from the relative lower punch displacement curve (RPD) taking into account the thermal expansion of the graphite tools. Densification starts at 1500 °C and reaches a maximal rate at 1900 °C. The fully dense specimens with finely equiaxed grains with average size of 4.05 ± 1.62 μm were obtained after an SPS treatment at 2200 °C with the heating rate 600 °C/min. The secondary phases at triple-junctions, which originated from the impurities of the starting boron carbide powder, were detected by TEM analysis, while HRTEM observation did not reveal any secondary phase films at the grain boundaries. It is suggested that the formation of the transient liquid phase stands behind the early stage of the densification. To summarize, boron carbide powders can self-bond without the assistance of additives by means of the SPS-processing at a faster and cheaper way and retain a fine grain structure.

Acknowledgment

This work was supported by the Israel Ministry of Science grant 3-3429.

References

[1] F. Thévenot, Boron carbide—a comprehensive review, Journal of the European Ceramic Society 6 (1990) 205–225.
[2] W.H. Kim, Y.H. Kohand, H.E. Kim, Densification and mechanical properties of B_4C with Al_2O_3 as a sintering aid, Journal of the American Ceramic Society 83 (2000) 2863–2865.
[3] V.J. Skorokhod, M.D. Vlajic, V.D. Krstic, Mechanical properties of pressureless sintered boron carbide containing TiB_2 phase, Journal of Materials Science Letters 15 (1996) 1337–1339.
[4] L. Schwetz, L. Sigl, L. Pfau, Mechanical properties of injection molded B_4C–C ceramics, Journal of Solid State Chemistry 133 (1997) 68–76.
[5] L.S. Sigl, Processing and mechanical properties of boron carbide sintered with TiC, Journal of the European Ceramic Society 18 (1998) 1521–1529.
[6] L. Levin, N. Frage, M.P. Dariel, Effect of Ti and TiO_2 additions on the pressureless sintering of B_4C, Metallurgical and Materials Transactions A 30 (1999) 3021–3210.
[7] H. Lee, R.F. Speyer, Hardness and fracture toughness of pressureless-sintered boron carbide (B_4C), Journal of the American Ceramic Society 85 (2002) 1291–1293.
[8] N.S. Brar, Z. Rosenberg, S.J. Bless, Applying Steinberg's model to the Hugoniot elastic limit of porous boron carbide specimens, Journal of Applied Physics 69 (1991) 7890–7891.
[9] D.E. Grady, Shock-wave strength properties of boron carbide and silicone carbide, Journal de Physique IV C8 (1994) 385–391.
[10] D.P. Dandekar, Shock response of boron carbide, ARL-TR-2456, 2001.
[11] H. Lee, R.F. Speyer, Pressureless sintering of boron carbide, Journal of the American Ceramic Society 86 (2003) 1468–1473.
[12] S.L. Dole, S. Prochazka, R.H. Doremus, Microstructural coarsening during sintering of boron carbide, Journal of the American Ceramic Society 72 (1989) 958–966.
[13] S. Prochazka, S.L. Dole, C.A. Hejna, Abnormal grain growth and microcracking in boron carbide, Journal of the American Ceramic Society 68 (1985) 235–236.
[14] K.A. Schwetz, W. Grellner, The influence of carbon on the microstructure and mechanical properties of sintered boron carbide, Journal of the Less-Common Metals 82 (1981) 37–47.
[15] B.R. Klotz, K.R. Cho, R.J. Dowding, Sintering aids in the consolidation of boron carbide (B_4C) by the plasma pressure compaction (P^2C) method, Materials and Manufacturing Processes 19 (2004) 631–639.
[16] G. Dipankar, S. Ghatu, S.S. Tirumalai, R. Ramachandran, G. Xin-Lin, Dynamic indentation response of fine-grained boron carbide, Journal of the American Ceramic Society 90 (2007) 1850–1857.
[17] U. Anselmi-Tamburini, A.Z. Munir, Y. Kodera, T. Imai, M. Ohyanagi, Influence of synthesis temperature on the defect structure of boron carbide: experimental and modeling studies, Journal of the American Ceramic Society 88 (2005) 1382–1387.
[18] N. Frage, S. Hayun, S. Kalabukhov, M.P. Dariel, The effect of Fe addition on the densification of B_4C powder by spark plasma sintering, Powder Metallurgy and Metal Ceramics 46 (2007) 533–538.
[19] G. Will, K.H. Kossobutzki, X-ray diffraction analysis of $B_{50}C_2$ and $B_{50}N_2$ crystallizing in the "tetragonal" boron lattice, Journal of the Less-Common Metals 47 (1976) 33–38.

[20] M.W. Chen, J.W. McCauley, K.J. Hemker, Microstructural characterization of commercial hot-pressed boron carbide ceramics, Journal of the American Ceramic Society 88 (2005) 1935–1942.
[21] B. Champagne, R. Anger, Mechanical properties of hot pressed B_4C materials, Journal of the American Ceramic Society 62 (1979) 149–153.
[22] D.R. Clarke, High-temperature microstructure of hot pressed silicon carbide, Journal of the American Ceramic Society 72 (1989) 1604–1609.
[23] X.F. Zhang, M.E. Sixta, L.C. De Jonghe, Grain boundary evolution in hot pressed ABC–SiC, Journal of the American Ceramic Society 83 (2000) 2813–2820.